Transient-State Kinetic Analysis of *Saccharomyces cerevisiae* MyristoylCoA:Protein *N*-Myristoyltransferase Reveals that a Step after Chemical Transformation Is Rate Limiting†

Thalia A. Farazi, Jill K. Manchester, and Jeffrey I. Gordon*

Department of Molecular Biology and Pharmacology, Washington University School of Medicine, St. Louis, Missouri 63110

Received September 1, 2000; Revised Manuscript Received October 11, 2000

ABSTRACT: MyristoylCoA:protein *N*-myristoyltransferase is a member of the superfamily of GCN5-related *N*-acetyltransferases and catalyzes the covalent attachment of myristate to the N-terminal Gly residue of proteins with diverse functions. *Saccharomyces cerevisiae* Nmt1p is a monomeric protein with an ordered bi-bi reaction mechanism: myristoylCoA is bound prior to peptide substrate; after catalysis, CoA is released followed by myristoylpeptide. Analysis of the X-ray structure of Nmt1p with bound substrate analogues indicates that the active site contains an oxyanion hole and a catalytic base and that catalysis proceeds through the nucleophilic addition−elimination mechanism. To determine the rate-limiting step in the enzyme reaction, pre-steady-state kinetic analyses were performed using a new, sensitive nonradioactive assay that detects CoA. Multiple turnover quenched flow studies disclosed that a step after the chemical transformation limits the overall rate of the reaction. Multiple and single turnover analyses revealed that the rate for the chemical transformation step is $13.8 \pm 0.6\ s^{-1}$ while the slower steady-state phase is $0.10 \pm 0.01\ s^{-1}$. Stopped flow kinetic studies of substrate acquisition indicated that binding of myristoylCoA to the apo-enzyme occurs through at least a two-step process, with a fast phase rate of $3.2 \times 10^8\ M^{-1}\ s^{-1}$ and a slow phase rate of $23 \pm 2\ s^{-1}$ (defined at 5 °C). Binding of an octapeptide substrate, representing the N-terminal sequence of a known yeast N-myristoylprotein (Cnb1p), to a binary complex composed of Nmt1p and a nonhydrolyzable myristoylCoA analogue (*S*-(*2*-oxo)pentadecylCoA) has a second-order rate constant of $2.1 \pm 0.3 \times 10^6\ M^{-1}\ s^{-1}$ and a dissociation rate of $26 \pm 15\ s^{-1}$ (defined at 10 °C). These results are interpreted in light of the X-ray structures of this enzyme.

Protein N-myristoylation refers to the cotranslational, covalent modification of eukaryotic and viral proteins with a rare 14-carbon saturated fatty acid, myristate. N-myristoylproteins have diverse functions and intracellular locations. Many N-myristoylproteins, including protein kinases, kinase substrates, and protein phosphatases, are involved in signal transduction cascades that affect a variety of cellular activities (reviewed in refs *1* and *2*). Myristate, which is attached via an amide bond to the N-terminal Gly of these proteins, promotes weak interactions with cellular membranes and/or other proteins that can be reversed at low thermodynamic cost (*1, 3*). Typically, N-myristoylproteins use an additional source of affinity to control their affiliation with protein partners or membranes. Some use so-called myristoyl-electrostatic switches: i.e., the hydrophobic interactions provided by myristate are supplemented by electrostatic interactions between positively charged protein side chains and negatively charged membrane phospholipid headgroups (*4, 5*). Other N-myristoylproteins use myristoyl-conformational switches that are "thrown" when a ligand is acquired or expelled, resulting in exposure or sequestration of the acyl chain (e.g., refs *6*−*8*). Reversible S-palmitoylation of some N-myristoylproteins containing an N-terminal Gly−Cys represents another type of switch that operates in several heterotrimeric G protein α-subunits, and appears to function as a signal for caveolar localization of some Src family tyrosine kinases (reviewed in ref *9*).

The essential contributions of N-myristoylproteins to eukaryotic cellular functions have been established by genetic studies. Protein N-myristoylation is catalyzed by enzyme myristoylCoA:protein N-myristoyltransferase (Nmt).[1] Loss-of-function mutations of *NMT* have revealed that this enzyme is essential for the survival of *Saccharomyces cerevisiae* (*10*−*13*) as well as *Candida albicans* and *Cryptococcus neoformans* (the two principal causes of systemic fungal infections in humans) (*14*−*16*).

NMT genes have been recovered and the primary structures of their protein products have been reported for these three organisms, plus *Histoplasma capsulatum* (*17*), *Plasmodium falciparum* (*18*), *Arabidopsis thaliana* (*19*), *Caenorhabditis elegans* (*20*), *Drosophila* melanogaster (*21*), *Mus musculus* (*22*), *Homo sapiens* (*22*), *Schizosaccharomyces pombe* (ac-

† This work was supported by a grant from the National Institutes of Health (AI38200).

* To whom correspondence should be addressed. Department of Molecular Biology and Pharmacology, Box 8103, Washington University School of Medicine, 660 So. Euclid Ave., St. Louis, MO 63110. Phone 314:362-7243. Fax: 314:362-7047. E-mail: jgordon@molecool.wustl.edu.

[1] Abbreviations: Nmt, myristoylCoA:protein *N*-myristoyltransferase; GNAT, GCN5-related *N*-acetyltransferase; NAD, nicotinamide adenine dinucleotide; DTT, dithiothreitol; HEPES, *N*-[2-hydroxyethyl]piperazine-*N*′-[2-ethanesulfonic acid].

10.1021/bi002074t CCC: $19.00
Published on Web 12/02/2000

cession number AL0022103) *Bos taurus* (AF232826 and AF223384) and *Candida glabrata* (AF073886).[2] *S. cerevisiae* Nmt1p was the first to be purified to homogeneity (*23*) and has been characterized extensively. This 455-residue monomeric enzyme has no known cofactor requirements. Nmt1p is highly selective for myristoylCoA in vitro and in vivo (*11*, *24*−*26*). Gly is invariably present at position 1, and Ser and Lys typically present at positions 5 and 6, respectively, of yeast N-myristoylproteins. Empirically derived rules for peptide recognition, based on an analysis of >100 synthetic peptides, have been used to scan the yeast genome for Nmt substrates. The results suggest that the genome encodes ∼70 N-myristoylproteins (∼1% of all yeast proteins; refs *1* and *12*). In vitro studies of yeast, fungal, and human Nmts have disclosed some divergence in their peptide specificites (*27*−*30*). These differences have been exploited to develop species-selective Nmt inhibitors that are fungicidal (*16*, *28*).

Steady-state kinetic studies of *S. cerevisiae*, *C. albicans*, and *H. sapiens* Nmts indicate that they have a sequential mechanism: the apo-enzyme binds myristoylCoA to form a Nmt1p·myristoylCoA binary complex that is competent to bind peptide substrate; after the ternary Nmt·myristoylCoA·peptide complex forms, catalytic transfer of myristate from CoA to the glycine amine occurs; CoA is then released, followed by myristoylpeptide (*30*−*32*).

Isothermal titration calorimetric and structural studies of *S. cerevisiae* and *C. albicans* Nmts have provided additional support for the ordered reaction mechanism. Calorimetry disclosed that apo-Nmt binds myristoylCoA but not peptide and that the binary Nmt1p·myristoylCoA complex is able to bind peptide substrates (*33*, *34*). The structures of two Nmts have been solved using X-ray crystallography. The *C. albicans* apo-enzyme structure has been refined to 2.45-Å resolution (ref *35*; protein data bank (PDB) accession number 1NMT). The structure of *S. cerevisiae* Nmt1p with a nonhydrolyzable myristoylCoA derivative, S-(*2-oxo*)pentadecylCoA, and a dipeptide inhibitor has been refined to 2.9-Å resolution (ref *36*; PDB accession number 2NMT). The Nmt fold consists of a large saddle-shaped β-sheet that is flanked on both of its faces by several helices. This fold places Nmt in the superfamily of GCN5-related *N*-acetyltransferases (GNAT; ref *37*) that includes histone *N*-acetyltransferase (*38*−*44*), aminoglycoside *N*-acetyltransferase (*45*, *46*), and serotonin *N*-acetyltransferase (*47*, *48*).

The Nmt fold has pseudo-2-fold symmetry: its N-terminal half forms the myristoylCoA binding site, while its C-terminal half forms most of the peptide binding site. Each of the symmetry related halves of Nmt is topologically equivalent to the monomer core structure of the GNAT superfamily members. A comparison of the structures of *C. albicans* apo-Nmt and the *S. cerevisiae* Nmt1p ternary complex indicates that the enzyme undergoes several conformational changes upon myristoylCoA binding, resulting in final assembly of a peptide binding site (ref *36*; see Discussion).

[2] Recent entries in GenBank from 9 other species have homology to these Nmts: *Strongyloides stercoralis* (BE580365), *Glycine max* (AW733718), *Gallus gallus* (AW355286), *Rattus sp.* (AW141188), *Lycopersicon esculentum* (AW036027), *Pleuronectes americanus* (AW013694), *Gossypium hirsutum* (AI726036), *Danio renio* (AI629225), and *Sus scrofa* (C94756).

Typically, acyl transfer reactions occur through the nucleophilic addition−elimination mechanism. Applying this mechanism to Nmt, catalytic transfer of a myristoyl moiety from CoA to a glycine amine would involve polarization of the thioester carbonyl to make the carbon attractive for nucleophilic attack and deprotonation of the glycine ammonium to generate a nucleophilic amine. The structure of the ternary Nmt1p complex supports this mechanism (*36*). Polarization of the carbonyl and transition state stabilization are apparently achieved by an oxyanion hole formed by backbone amide groups of Phe170 and Leu171, while the carboxylate of the C-terminal Leu455 residue appears to be involved in generation of the nucleophilic amine.

With these structural findings in mind, we have now performed a series of pre-steady-state kinetic analyses to define the rate of the chemical transformation step and to determine whether this, or another step, is rate-limiting for the Nmt1p reaction.

MATERIALS AND METHODS

Materials. Enzymes were purchased from Boehringer Mannheim, with the exception of *Leuconostoc mesenteroides* glucose-6 phosphate dehydrogenase, which was obtained from Calbiochem. All other biochemical reagents were from Sigma.

Purification of S. cerevisiae Nmt1p. Nmt1p was expressed in *Escherichia coli* (*49*) and purified to apparent homogeneity, free of thioesterase activity, using methods described in a previous publication (*34*). The concentration of the purified enzyme in storage buffer [50 mM HEPES (pH 7.5), 15 mM EDTA] was defined (*50*) (molar extinction coefficient 63 163 M^{-1} cm^{-1} at 280 nm).

Pre-Steady-State Nmt1p Assay. Overview. This new assay is based on measurement of CoA, the first product released by Nmt1p. The assay includes the following steps: (a) reaction initiation; (b) quenching of the reaction with perchloric acid; (c) conversion of CoA to NAD^+ (see Scheme 1 in Figure 1, panel A), followed by (d) amplification NAD^+ with the associated production of lactone, (e) nonenzymatic conversion of lactone to 6-phosphogluconate (6-PG), (f) enzymatic conversion of 6-PG (with addition of $NADP^+$), to ribulose-5-phosphate and NADPH, and finally measurement of NADPH fluorescence (see Scheme 2 in Figure 1, panel A). The general principles underlying the use of pyridine nucleotide-based enzymatic cycling to achieve analytic sensitivity have been described extensively by Lowry and co-workers, and applied to a wide variety of biological systems (reviewed in ref *51*).

Specific Details. To perform the assay, 45-μL samples were assembled, one containing 0.6−2 μM of purified Nmt1p and the other 1−30 μM of an octapeptide substrate and myristoylCoA. Both samples contained 10 mM Tris-HCl (pH 8.1), 5 mM $MgCl_2$, 0.5 mM DTT, and 0.1 mM EDTA. Following a 10-min pre-equilibration at 24 °C, the two samples were mixed using a Rapid Quenched-Flow apparatus (KinTek Corporation, Austin, TX). The reaction was quenched at various times after initiation (10 ms to 60 s) by adding 0.2 mL of 0.15 M perchloric acid. A sample without peptide was used as a reference negative control.

The quenched samples were centrifuged at 12000*g* for 2 min at room temperature to pellet precipitated protein. A

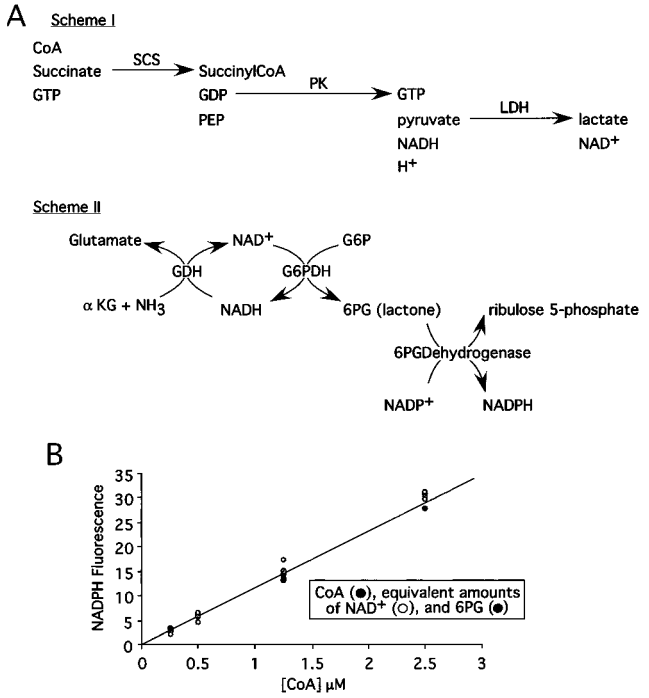

FIGURE 1: Detecting CoA, the first product released by Nmt, using pyridine nucleotide-based enzymatic cycling to achieve analytic sensitivity. (A) Cycling schemes. Scheme 1 yields NAD^+ from CoA; Scheme 2, amplification of NAD^+. See text for further details. SCS, succinylCoA synthetase; PEP, phosphoenolpyruvate; PK, pyruvate kinase; LDH, lactate dehydrogenase; αKG, α-ketoglutarate; G6P, glucose 6-phosphate; 6PG, 6-phosphogluconate; GDH, glutamate dehydrogenase; G6PDH, glucose 6-phosphate dehydrogenase. (B) Evidence for the linearity of the detection scheme. Reaction mixtures lacking Nmt1p were assembled. Defined amounts of CoA standards, or equivalent amounts of NAD^+ or 6PG, were added at the appropriate assay step in the schemes described in panel A. The reactions were followed to completion. The data illustrate that for the range of CoA produced during the course of the pre-steady-state analyses, the cycling procedure (and final conversion of 6PG to NADPH) yields products in amounts that are linearly related to the input concentration of substrates.

0.1-mL aliquot was then removed and neutralized with 10 μL of a solution containing 1.03 N KOH, 0.55 M Tris-HCl (pH 8.1), and 2.2 μM *S*-(*2*-oxo)pentadecyl-CoA, a potent competitive inhibitor of Nmt1p (K_i = 5 nM; ref *34*). The inhibitor was included to ensure that there would be no residual Nmt1p activity during the subsequent steps of the CoA detection assay.

Twenty five microliters of CoA reagent was then added [CoA reagent = 250 mM Tris-succinate (pH 7.7), 25 mM $MgCl_2$, 2.5 mM DTT, 0.5 mM EDTA, 0.5 mM phosphoenolpyruvate, 50 μM GTP, 10 μM NADH, 30 μg/mL beef heart lactate dehydrogenase (EC 1.1.1.27; specific activity = 0.6 U/μg), 600 μg/mL rabbit muscle pyruvate kinase (EC 2.7.1.40; 0.2 U/μg), and 50 μg/mL pig heart succinylCoA synthetase (EC 6.2.1.4; 0.01 U/μg)]. The solution was incubated at 24 °C for 20 min, and the reaction was terminated by addition of 10 μL of 2N HCl (to destroy enzymatic activity and to eliminate excess NADH). A 4-μL aliquot was removed and transferred to 0.1 mL of pyridine nucleotide cycling reagent [cycling reagent = 50 mM imidazole-HCl (pH 7.0), 7.5 mM α-ketoglutarate, 5 mM glucose-6-phosphate, 25 mM ammonium acetate, 0.02% bovine serum albumin (fraction V from Sigma), and 0.1 mM ADP]. Our Nmt1p reactions produced 0.05−3 μM of CoA product depending upon the length of the incubation. To detect CoA in the range of 0.05−1 μM, the cycling reagent contained 400 μg/mL glutamate dehydrogenase (EC 1.4.1.2; 0.12 U/μg), and 80 μg/mL *Leuconostoc mesenteroides* glucose-6-phosphate dehydrogenase (EC 1.1.1.49; 0.2 U/μg). Over the course of a 60-min incubation at 38 °C, the cycling reaction will produce a 10000-fold amplification of NAD^+ according to Scheme 2 in Figure 1, panel A. To detect CoA in the range 1−3 μM, we reduced the concentration of each of the two enzymes in the cycling reagent by 50% so that a 5000-fold amplification would be achieved.

The validity of the assay was assessed by performing a series of control experiments. Omitting either the myristoyl-CoA or the octapeptide substrates failed to produce detectable product and provided a reference blank. When the perchloric acid quenching solution was added together with Nmt1p prior to addition of substrates, no product was detected even after a 1-h incubation, establishing the completeness of the quench. CoA (0.2−0.5 μM) was added directly to quench solution, and all subsequent steps in the detection scheme were performed. The results indicated that the perchloric acid had no effect on the stability of CoA. Finally, addition of myristoylCoA to the quench solution did not produce detectable hydrolysis to CoA.

The linearity of the detection scheme over the range of 0.05−3 μM CoA was established by performing reactions in the absence of Nmt1p. Additional validation was obtained by omitting all steps prior to cycling (i.e., Scheme 2) and then adding NAD^+ or 6PG at levels that are equivalent to what would have been produced at this stage of the assay by 0.05−3 μM CoA.

The amount of CoA produced was calculated as follows. NADPH produced from the final step of Scheme 2 was detected fluorometrically (excitation = 360 nm; emission = 460 nm). The results were referenced to a series of external control reactions where Nmt1p was omitted and defined amounts of CoA were added prior to performing the reactions in Schemes 1 and 2. All assays were performed in duplicate. The amount of CoA produced was plotted versus time and fit to eq 1.

$$[\mathrm{CoA}] = A(1 - e^{-k_b t}) + k_{ss} t \qquad (1)$$

where A is the amplitude of the single exponential (burst phase), k_b is the burst rate, and k_{ss} is the steady-state rate. [For single turnover experiments, the second term of eq 1 was omitted. The kinetic parameters A, k_b, and k_{ss} were calculated using nonlinear least-squares analysis (program Scientist; Micromath, Salt Lake City, UT)].

Equilibrium Fluorescence Measurements of the Binding of MyristoylCoA to Nmt1p. The dissociation constant of Nmt1p for myristoylCoA was determined as follows. A solution was prepared containing 100 or 200 nM Nmt1p, 20 mM HEPES (pH 7.5), 50 mM NaCl, and varying amounts of myristoylCoA (5−300 nM). Following pre-equilibration at 20 °C for 5 min, the time course of fluorescence change was recorded using a stirred 3-mL cuvette and a PTI Photon Technology fluorimeter [excitation = 295 nm (2 nm slit); emission = 330 nM (5 nm slit)]. Corrections for the inner filter effect were unnecessary because the optical densities at 295 nm for all solutions were well below 0.05 absorbance units (*52*). The extent of tryptophan fluorescence quenching,

Q_{obs}, was plotted as a function of the total substrate concentration. Q_{obs} was calculated from eq 2.

$$Q_{obs} = |(F_{init} - F_{obs})|/F_{init} \quad (2)$$

where F_{init} is the initial fluorescence before addition of myristoyCoA at the specific Nmt1p concentration, and F_{obs} is the fluorescence intensity measured at specific myristoyl-CoA concentrations. The titration data were fit to a one site binding scheme using Scientist.

Stopped Flow Analysis of the Rate of Binding of Substrates to Nmt1p. Reaction rate measurements were performed using a stopped flow apparatus from Applied Photophysics (Surrey, United Kingdom) operating in the fluorescence mode (excitation = 295 nm; emission monitored at >305 nm). The binding reaction was performed in the same buffer as that used for the equilibrium fluorescence measurements. When assaying the binding of myristoylCoA, thioesterase-free apo-Nmt1p (100−300 nM) was reacted with myristoylCoA (0.3−8 μM) at 5, 10, and 20 °C. When monitoring the binding of an octapeptide substrate, a binary complex of Nmt1p and *S*-(*2*-oxo)pentadecylCoA was pre-formed by incubating Nmt1p (200 nM) and S-(*2*-oxo)pentacylCoA (2 μM) for 5 min at 10 °C, followed by addition of GAAPSKIV-NH_2 (12.5−200 μM).

Fluorescence (Fl) was plotted versus time and fit either to a single or a double exponential with a floating end point according to eq 3.

$$Fl = Ae^{-k_1 t} + Be^{-k_2 t} + C \quad (3)$$

Rates (k_1 and k_2), amplitudes (*A* and *B*), and the endpoint (*C*) were estimated using nonlinear least-squares analysis (Scientist).

RESULTS

The Rate-Limiting Step in the Nmt Reaction Occurs after the Chemical Transformation. We conducted transient state kinetic analyses to examine whether the chemical transformation step is the rate-limiting step in the Nmt1p reaction (*53*). To do so, we developed a new, rapid, nonradioactive assay of Nmt activity that has great sensitivity. The assay is based on measurement of CoA, the first product released by the enzyme. Sensitivity is achieved through pyridine-nucleotide-based amplification using Schemes 1 and 2 shown in Figure 1, panel A, and the protocol described in Materials and Methods. Control experiments confirmed that the assay is Nmt1p-dependent (see Materials and Methods) and that detection of CoA is linear in the range of product formed under the conditions of the pre-steady-state assay (e.g., Figure 1, panel B). Moreover, when a limiting amount of myristoylCoA is added to the reaction, the amount of CoA released is equivalent to the input level of the acylCoA (see below).

Pre-steady-state analyses were performed at saturating levels of myristoylCoA and GAAPSKIV-NH_2, an octapeptide substrate derived from the N-terminus of Cnb1p. Cnb1p is a yeast N-myristoylprotein homologous to the regulatory component of the mammalian Ca^{2+}/calmodulin-dependent phosphoprotein phosphatase calcineurin B (*54*). The K_d of myristoylCoA for apo-Nmt1p, and of GAAPSKIV-NH_2 for a binary complex of Nmt1p and a nonhydrolyzable myristoylCoA analogue, have been defined by isothermal titration calorimetry (15 nM and 4 μM, respectively; refs *33* and *34*). The concentration of each of these substrates in the pre-steady-state assay was 20 μM. Under these conditions, in the absence of any preincubation of myristoylCoA with apoNmt1p, a burst in product (CoA) formation would indicate that a step after catalysis (chemical transformation) is at least partially rate-limiting in the Nmt1p reaction.

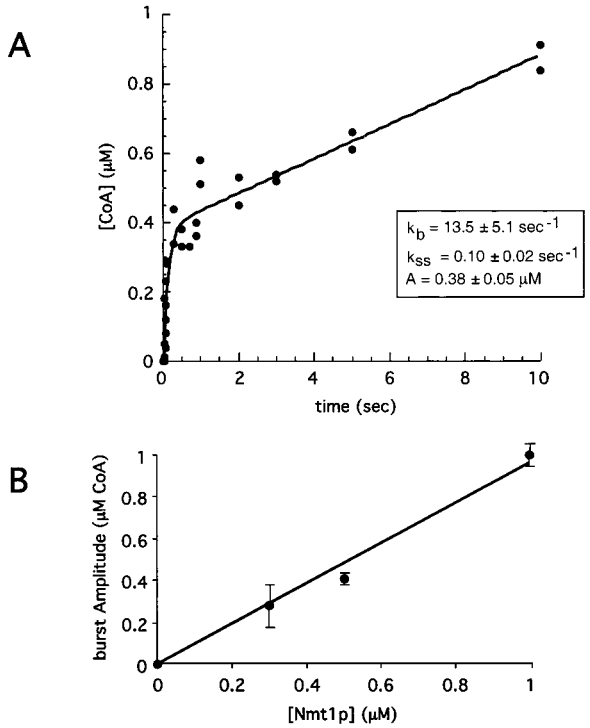

FIGURE 2: Multiple turnover pre-steady-state kinetic analysis of Nmt1p. (A) A representative quenched flow study performed at 24 °C: [Nmt1p] = 0.5 μM; [myristoylCoA] = 20 μM; [GAAPSKIV-NH_2] = 20 μM. CoA product formation is plotted as a function of reaction time. The data were fit using eq 1 described in the text. k_b, burst rate; *A*, burst amplitude; k_{ss}, steady-state rate. (B) Linear relationship between the burst amplitude and the concentration of Nmt1p used in pre-steady-state assays. Both substrates were at 20 μM. Mean values ± SE are plotted (two independent experiments, each performed in duplicate).

Initial pre-steady-state experiments employed 0.5 μM Nmt1p and 20 μM each of myristoylCoA and the Cnb1p octapeptide. The reaction (performed at 24 °C) was initiated by addition of both substrates and stopped 40 ms to 60 s later with perchloric acid, using a quenched flow apparatus. The time course of CoA production was biphasic. There was a fast burst phase of 13.5 ± 5.1 s^{-1} (95% confidence interval), followed by a slower steady-state phase of 0.10 ± 0.02 s^{-1} (Figure 2). To establish that the burst amplitude was proportional to the Nmt1p concentration, the pre-steady-state analyses were repeated using 0.3 and 1.0 μM Nmt1p (each experiment in duplicate). Figure 2, panel B, shows the linearity of the burst amplitude as a function of [Nmt1p]. The mean value (± SE) of the burst phase, calculated from these experiments using different Nmt1p concentrations, is 13.8 ± 0.6 s^{-1}, while the slower steady-state phase is 140-fold slower (0.10 ± 0.01 s^{-1}).

Since the substrate concentrations exceeded the concentration of Nmt1p in the pre-steady-state experiments shown in Figure 2, multiple turnovers were allowed. Determination of the burst phase rate in multiple turnover pre-steady-state

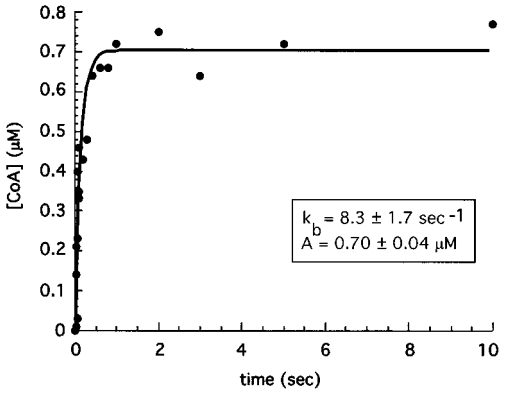

FIGURE 3: Single turnover pre-steady-state kinetic analysis. A representative quenched flow study conducted at 24 °C: [Nmt1p] = 1 μM; [myristoylCoA] = 0.8 μM; [GAAPSKIV-NH_2] = 15 μM. Data were fit as described in Materials and Methods. Two independent experiments yielded an average value of 12.6 ± 4.3 s^{-1} for the rate.

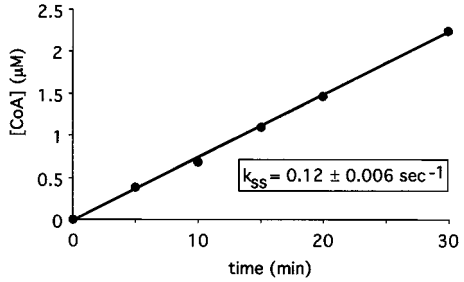

FIGURE 4: Steady-state kinetic analysis of Nmt1p. Assays were performed at 24 °C using 10 nM Nmt1p and 20 μM substrates.

experiments can, in theory, be confounded by a number of factors (e.g., product inhibition, problems with accurate determination of rate constants from biphasic time course data). Therefore, we analyzed the burst rate using single turnover experiments. These experiments were performed by first preincubating apo-Nmt1p (1 μM) with myristoylCoA, at a concentration of acylCoA that was less than the concentration of enzyme (i.e., 0.8 μM). The reaction was then initiated by addition of saturating amounts of the octapeptide substrate (15 μM). The single turnover results (Figure 3) revealed a rate of 12.6 ± 4.3 s^{-1} (n = 2 experiments), a value that is in good agreement with the burst rate defined from the multiple turnover transient kinetic analysis. Since the single turnover experiment was performed after preincubating apoNmt1p with myristoylCoA, while the multiple-turnover pre-steady-state experiments were performed without preincubation, the similarities in the calculated rate of the first turnover suggests that the rate of myristoylCoA binding is not the limiting step in the enzyme reaction (see next section).

We also evaluated the accuracy of the slower steady-state phase calculated from the pre-steady-state experiments shown in Figure 2. We did so by performing a "steady" state analysis in which 20 μM myristoylCoA and 20 μM octapeptide were added to 10 nM apo-Nmt1p, and CoA formation was monitored over a course of a 30-min reaction. The results (Figure 4) indicated that the steady-state rate was 0.12 ± 0.006 s^{-1}, a value in excellent agreement with the value obtained from the pre-steady-state study (0.10 ± 0.01 s^{-1}).

Stopped-Flow Kinetic Analyses of the Rate of Binding of MyristoylCoA to apo-Nmt1p. Stopped flow studies were performed to investigate the kinetics of myristoylCoA binding to apo-Nmt1p. Previous studies had shown that binding of myristoylCoA to apo-Nmt1p results in a readily detectable quenching of the enzyme's intrinsic tryptophan fluorescence (*31*). Stopped flow analyses were performed at 50 mM NaCl, which stabilizes the intrinsic tryptophan fluorescence of the apo-enzyme throughout the time course of the experiment. Titration of apo-Nmt1p with increasing concentrations of myristoylCoA yields a K_d of 2.6 ± 1.4 nM (data not shown). At 20 °C, using 100 or 200 nM apo-Nmt1p and at least a 5-fold molar excess of myristoylCoA (to ensure pseudo-first-order conditions), the time course of fluorescence quenching followed a single exponential, described by a rate of 107 ± 14 s^{-1} (n = 4) (data not shown). This rate was independent of myristoylCoA concentration (0.5−8 μM).

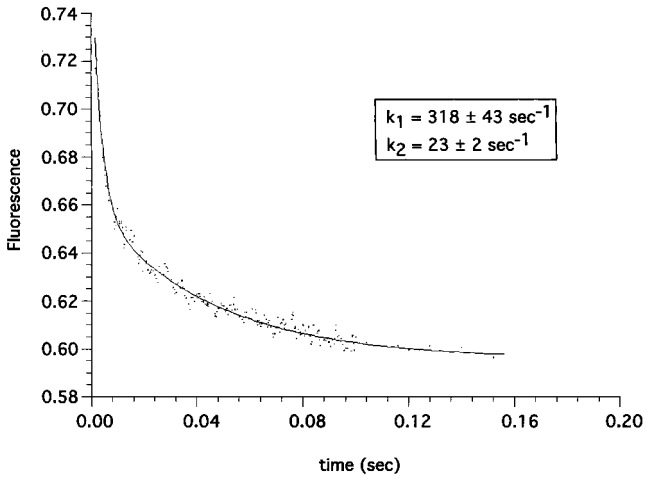

FIGURE 5: Stopped flow kinetic study of the rate of binding of myristoylCoA to apo-Nmt1p. Analysis conducted at 5 °C using 200 nM thioesterase-free apo-Nmt1p, and 1 μM myristoylCoA. Data were fit to a double exponential. k_1, fast phase; k_2, slow phase.

The amplitude (A) of the single-exponential describing the time course of the fluorescence quenching did not extrapolate back to the fluorescence of the apo-enzyme, which implies that another process leading to fluorescence quenching was occurring during the 1.5-ms period between sample mixing and when the instrument begins to collect data (i.e., a rate greater than 600 s^{-1} cannot be determined). To characterize this fast process, we performed the stopped-flow experiments at 10 and 5 °C. At 5 °C and at the lowest concentration of myristoylCoA tested (1 μM), we observed a time course of binding that was fitted best to a double exponential, with a fast phase rate of 318 ± 43 s^{-1} and a slow phase rate of 23 ± 2 s^{-1} (Figure 5). The sum of the amplitudes of these fast and slow phases extrapolate to the fluorescence of the apo-enzyme. It was not possible to accurately determine the rate of the fast phase at higher concentrations of myristoylCoA.

Together, these results suggest that binding of myristoyl-CoA is a two-step process. The fast phase is most likely diffusion controlled (i.e., its rate is 3.2 × 10^8 M^{-1} s^{-1}). Potential explanations for the slow phase are provided in the Discussion.

Stopped-Flow Kinetic Analyses of the Rate of Binding of an Octapeptide Substrate to S-(2-Oxo)pentadecylCoA:Nmt1p Complex. To investigate the kinetics of binding of an octapeptide substrate to the binary Nmt1p complex, we

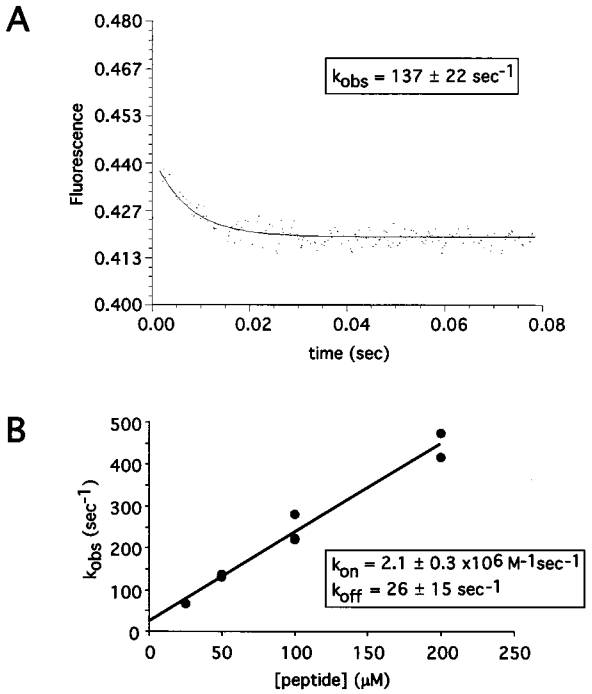

FIGURE 6: Stopped flow kinetic study of the rate of binding of GAAPSKIV-NH_2 to a preformed binary complex of Nmt1p and a nonhydrolyzable myristoylCoA analogue. (A) Results from a representative study conducted at 10 °C using 200 nM Nmt1p complexed with *S*-(2-oxo)pentadecylCoA and 50 μM of the octapeptide substrate. The data were fit to a single exponential. k_{obs}, observed rate. (B) k_{obs} plotted as a function of the concentration of GAAPSKIV-NH_2. The intercept corresponds to the dissociation rate constant (k_{off}). The slope corresponds to the second-order rate constant (k_{on}).

performed stopped flow analysis using a myristoylCoA analogue, *S*-(*2*-oxo)pentadecylCoA (*55*). *S*-(*2*-oxo)pentadecylCoA is a competitive inhibitor of the enzyme: it contains an additional methylene interposed between the fatty acid carbonyl and the thioester sulfur, creating a nonhydrolyzable thioether. Isothermal titration calorimetry has established that the thermodynamics of binding of this analogue to apo-Nmt1p are virtually identical to that of myristoylCoA (*34*). The affinity of the analogue for the apo-enzyme was 3 nM, based on calorimetry.

Apo-Nmt1p (200 nM) was pre-equilibrated with 2 μM *S*-(*2*-oxo)pentadecylCoA and increasing concentrations of GAAPSKIV-NH_2 (12.5−200 μM) were added. The time course was best described by a single exponential (Figure 6, panel A). When the observed rate (k_{obs}) was plotted as a function of octapeptide concentration, the second-order rate constant k_{on} was calculated to be 2.1 ± 0.3 × 10^6 M^{-1} s^{-1} (Figure 6, panel B). The intercept of this plot corresponds to the dissociation rate constant, k_{off} (26 ± 15 s^{-1}). On the basis of the experimentally determined k_{on} and k_{off} values, we estimated that the K_d for binding of the octapeptide was 12 μM, in agreement with the previously published calorimetric data (*33*). Together, these results suggest that the binding of this octapeptide substrate to the binary Nmt1p complex, is a single step process that is most likely diffusion controlled.

Determination of the Rate of the Chemical Transformation. Single turnover experiments were performed by first preincubating 0.5 μM apo-Nmt1p with 0.5 μM myristoylCoA and then adding different concentrations of the octapeptide substrate (0.5−15 μM). The kinetic data were globally fitted to the following minimal kinetic scheme using FITSIM (*56*).

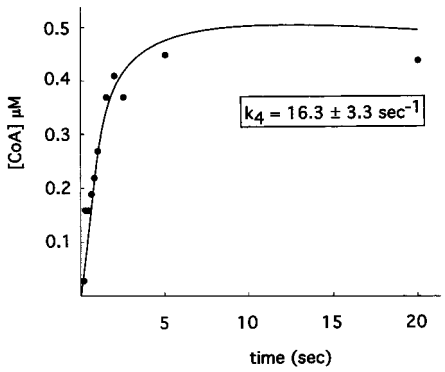

FIGURE 7: Calculating the rate of the chemical transformation step from single turnover pre-steady-state kinetic analyses. Representative quenched flow study, performed at 24 °C using 0.5 μM Nmt1p, 0.5 μM myristoylCoA, and 1 μM GAAPSKIV-NH_2. Data were fit as described in the text. k_4, rate of chemical transformation.

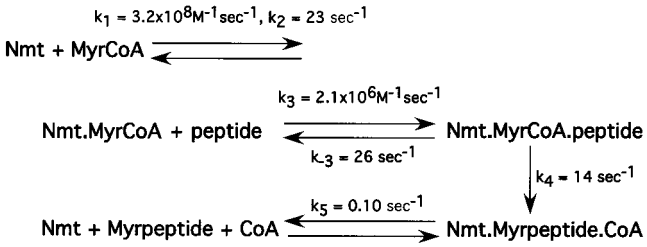

FIGURE 8: Kinetic mechanism and rate constants. Rate constants shown are taken from the experiments shown in Figures 2−7. k_1 and k_2 were determined at 5 °C. Note that k_2 was also determined at 20 °C (107 ± 14 s^{-1}). k_3 and k_{-3} were determined at 10 °C, while k_4 and k_5 were determined at 24 °C.

$$\text{Nmt·MyrCoA} + \text{peptide} \underset{k_{-3}}{\overset{k_3}{\rightleftharpoons}} \text{Nmt·MyrCoA·peptide} \xrightarrow{k_4} \text{Nmt·Myrpeptide·CoA}$$

k_3 was fixed in FITSIM as diffusion limited (2.1 × 10^6 M^{-1} s^{-1}) based on the stopped flow data. k_{-3} was fixed at 26 s^{-1}, also based on the stopped flow analysis. k_{-4} was fixed as 0 (assuming that catalysis is irreversible; see ref *31*). The rate of the chemical transformation, k_4, was calculated to be 16.3 ± 3.3 s^{-1} (Figure 7). This is in good agreement with the burst rate determined from the multiple turnover pre-steady-state experiments and the rate defined from the earlier single turnover experiment (performed at saturating octapeptide concentration and fitted to a single exponential).

DISCUSSION

Figure 8 summarizes the results of these kinetic analyses of the Nmt1p reaction. Our studies indicate that a step after the chemical transformation serves to limit the rate of the acyltransferase. There is a 140-fold difference between the rate of the chemical transformation and the steady-state rate. This finding is consistent with observations made from a comparison of the *C. albicans* apo-Nmt structure and the structure of Nmt1p with bound substrate analogues. These comparisons suggest that, following catalysis, the enzyme undergoes a number of conformational changes to allow release of the myristoylpeptide product.

Figure 9 shows the structure of Nmt1p with bound substrate analogues and points out areas of the structure

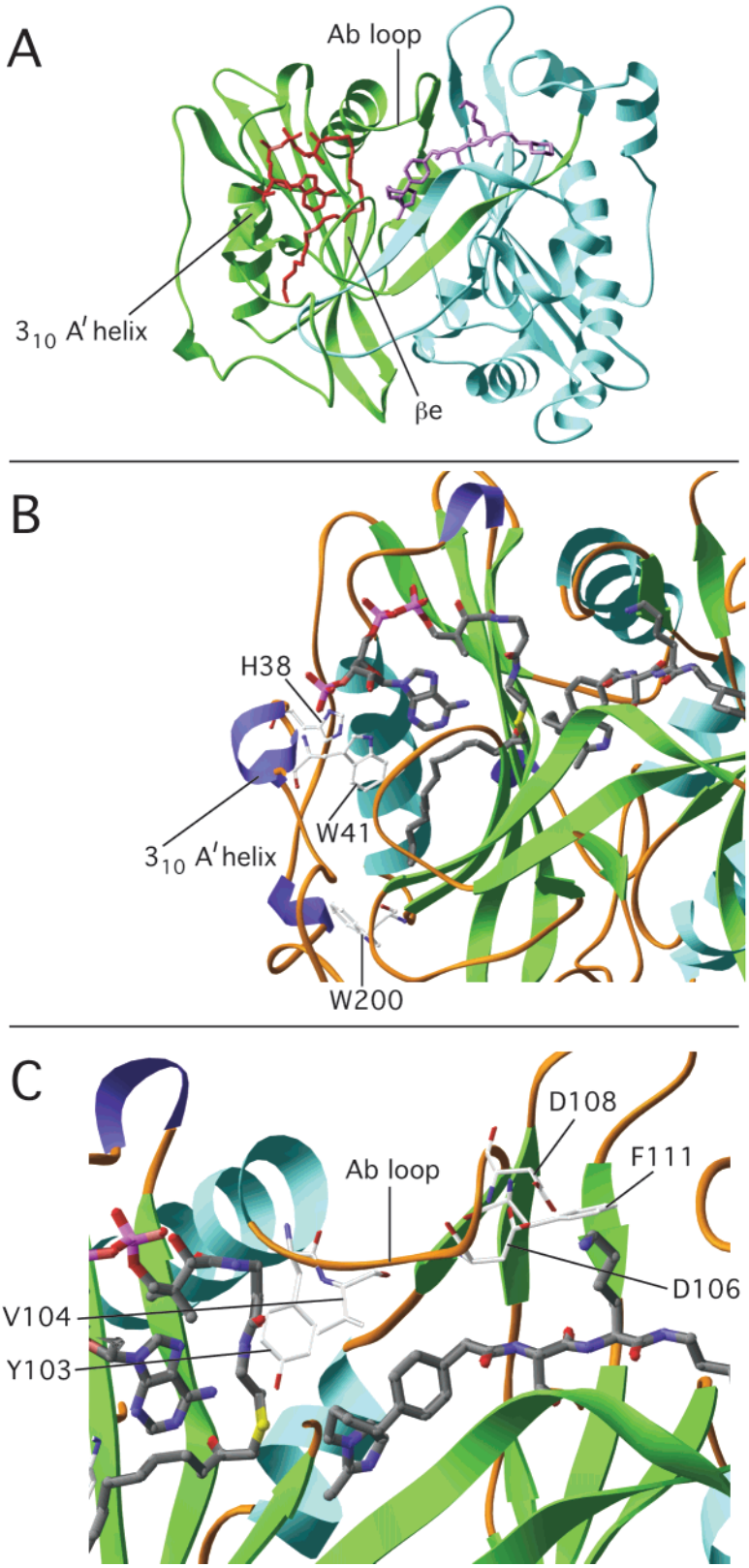

FIGURE 9: Structure of Nmt1p with bound substrate analogues. (A) Ribbon diagram of Nmt1p with bound *S*-(2-oxo)pentadecylCoA (red) and the dipeptide inhibitor SC-58272 (lavender). The N-terminal symmetry-related half (A34 to N225) is colored green. The C-terminal symmetry related half (W226 to L455) is colored blue. Residues 1−33 of Nmt1p are disordered in the ternary complex. (B) MyristoylCoA binding site. Note the 3_{10} A′ helix, which is ordered upon binding of myristoylCoA, including residues H38 and W41. W200 is located at the bottom of the acylCoA binding pocket. (C) The "bifunctional" Ab loop involved in binding of acylCoA and peptide substrates. Y103 and V104 make contacts with the pantetheine group of the bound acylCoA. D106, D108, and F111 interact with the Lys residue retained in the dipeptide competitive inhibitor SC-58272. Atom color code in panels B and C: oxygen, red; phosphorus, pink; carbon, silver; nitrogen, purple; sulfur, yellow.

whose conformations are likely affected by acquisition and/or release of substrates. An N-terminal 3_{10} helix is present in the ternary complex (*36*) but is absent in the apo-enzyme (*35*), suggesting that the helix is ordered by myristoylCoA.

Figure 9, panel B, presents some of the contacts between this helix (designated A′), elements of CoA (3′-phosphate, N3 of adenine, 2′-hydroxyl of the pentose sugar), and the myristoyl chain. We have recently solved the structure of Nmt1p with bound myristoylCoA to 2.2-Å resolution (Farazi, T., Waksman, G. and Gordon, J. I., manuscript submitted). This structure provides further and more direct evidence that myristoylCoA binding structures the 3_{10} helix.

Figure 9, panel C shows the Ab loop. In the 2.45-Å resolution structure of *C. albicans* apo-Nmt, this loop displays conformational heterogeneity. In the structure of the *S. cerevisiae* ternary complex, the Ab loop is ordered and makes contacts with pantetheine of the bound nonhydrolyzable myristoylCoA analogue and with Lys of the bound dipeptide inhibitor. The structure of the ternary complex indicates that residues in the Ab loop contribute substantially more buried surface area to binding of the peptide analogue than to binding of the nonhydrolyzable myristoylCoA analogue (*36*).

On the basis of these observations, we proposed (*36*) the following steps in the Nmt1p reaction: (a) myristoylCoA binding induces conformational changes affecting the 3_{10} A′ helix; (b) restructuring of the Ab loop permits binding of a peptide substrate to the "cryptic" peptide binding site; (c) following catalytic transfer of myristate from CoA to the glycine amine, CoA is able to depart from the ternary complex; (d) once CoA exits, the Ab loop reverts to a more flexible state and the 3_{10} A′ helix loses critical contacts required to maintain its secondary structure; (e) freed from its interactions with the Ab loop and a substantial portion of the acyl chain binding pocket provided by the A′ helix, myristoylpeptide is released. The pre-steady-state kinetic studies described in this report indicate that steps c−e are limiting in the Nmt reaction.

The acylCoA binding site of Nmt1p contains two tryptophans that have contacts with myristoylCoA: (i) W41 of the A′ helix (contacts with the 3′-phosphate of CoA; N3 of adenine, and C6 of myristate); (ii) W200, a component of the floor of the acyl chain binding site (contacts with the ω-terminal methyl of myristate). The stopped flow fluorescence analysis reported above suggests that myristoylCoA binding occurs as a two-step process. As noted in Results, the fast phase is most likely diffusion controlled (i.e., its rate is 3.2×10^8 M^{-1} s^{-1}). Our studies do not allow distinction between two schemes that could describe the observed biphasic behavior: (i) an isomerization step follows binding of myristoylCoA; (ii) Nmt exists in two different conformations, one of which preferentially binds myristoylCoA:

$$\mathrm{E + MyrCoA} \rightleftharpoons \mathrm{E.MyrCoA} \rightleftharpoons \mathrm{E^*.MyrCoA}$$

$$\mathrm{E^* + MyrCoA} \rightleftharpoons \mathrm{E^*.MyrCoA}$$

$$\mathrm{E}$$

Finally, it is important to note that the minimal kinetic scheme presented in Figure 8 does not include a step for conformational changes that may occur after formation of the ternary complex. Moreover, our pre-steady-state kinetic experiments cannot distinguish between the possibility that the burst rate corresponds to the rate of a conformational change after formation of the ternary complex or the actual chemical reaction.

Nmt and the GNAT Superfamily. As noted in the introduction, Nmt has structural homology to members of the GNAT superfamily that catalyze the transfer of the acetyl moiety from CoA to a primary amino group of various targets (i.e., histones, aminoglycoside antibiotics, serotonin). Nmt, histone *N*-acetyltransferase, and serotonin *N*-acetyltransferase are the most thoroughly characterized members of the GNAT family: each has been subjected to structural, steady-state kinetic, and mutagenesis analyses. The catalytic mechanism proposed for all three enzymes is similar: direct nucleophilic attack of the substrate primary amine at the reactive thioester bond of the acylCoA. Chemical transformation is aided by two elements located in the active sites of these three enzymes: a catalytic base, which by abstracting a proton from the primary amine makes it a better nucleophile, and an oxyanion hole that polarizes the reactive thioester carbonyl (*36*, *39*, *47*).

Like Nmt, serotonin *N*-acetyltransferase follows an ordered reaction pathway. This conclusion is based on steady-state inhibition studies (*57*), as well as a comparison of the structures of the enzyme without substrates, and with a bound bisubstrate analogue (*48*). On the basis of their structural studies, Hickman and co-workers have concluded that acetylCoA binding restructures an N-terminal loop into α-helix. The restructuring affects ~20 residues that includes a region located in the conserved motif C found in GNAT family members.[3] AcetylCoA binding to serotonin *N*-acetyltransferase "unveils" a cryptic binding site for serotonin (*48*).

Comparisons of the structures of histone *N*-acetyltransferase without substrates, with bound acetylCoA, and with bound CoA/histone H3 also indicate that acetylCoA acquisition is necessary to create a functional binding site for the second substrate (i.e., histone H3; ref *39*).

Nmt represents the only GNAT where pre-steady-state studies are available. Steady-state viscosity experiments, employing natural substrates, suggest that diffusional release of product is the principal rate-determining step for serotonin *N*-acetyltransferase (*58*). The rate-limiting step for histone *N*-acetyltransferase has not been reported. Pre-steady-state studies, employing the sensitive CoA-based assay described in this paper, can now be applied to other GNAT family members to determine whether the steps after chemical transformation serve to limit their reactions.

ACKNOWLEDGMENT

We thank Carl Frieden and Timothy Lohman and members of their labs for helpful suggestions during the course of these studies.

REFERENCES

1. Bhatnagar, R. S., Ashrafi, K., Futterer, K., Waksman, G., and Gordon, J. I. (2000) in *The Enzymes: Protein Lipidation* (Tamanoi, F., and Sigman, D. S., Eds.) pp 241−290, Academic Press, Inc., San Diego, California.

[3] Motif C is represented in the N-terminal half of Nmt1p as strand a and helix A and in the C-terminal half as strand h and helix F (reviewed in ref *1*).

2. Boutin, J. A. (1997) *Cell Signal 9*, 15−35.
3. Peitzsch, R. M., and McLaughlin, S. (1993) *Biochemistry 32*, 10436−43.
4. McLaughlin, S., and Aderem, A. (1995) *Trends Biochem. Sci. 20*, 272−6.
5. Murray, D., Hermida-Matsumoto, L., Buser, C. A., Tsang, J., Sigal, C. T., Ben-Tal, N., Honig, B., Resh, M. D., and McLaughlin, S. (1998) *Biochemistry 37*, 2145−59.
6. Zozulya, S., and Stryer, L. (1992) *Proc. Natl. Acad. Sci. U.S.A. 89*, 11569−73.
7. Ames, J. B., Ishima, R., Tanaka, T., Gordon, J. I., Stryer, L., and Ikura, M. (1997) *Nature 389*, 198−202.
8. Goldberg, J. (1998) *Cell 95*, 237−48.
9. Linder, M. E. (2000) in *The Enzymes: Protein Lipidation* (Tamanoi, F., and Sigman, D. S., Eds.) pp 215−240; Academic Press, Inc., San Diego, California.
10. Duronio, R. J., Towler, D. A., Heuckeroth, R. O., and Gordon, J. I. (1989) *Science 243*, 796−800.
11. Duronio, R. J., Rudnick, D. A., Johnson, R. J., Johnson, D. R., and Gordon, J. I. (1991) *J. Cell Biol. 113*, 1313−1330.
12. Ashrafi, K., Farazi, T. A., and Gordon, J. I. (1998) *J. Biol. Chem. 273*, 25864−74.
13. Ashrafi, K., Lin, S. S., Manchester, J. K., and Gordon, J. I. (2000) *Genes Dev. 14*, 1872−85.
14. Weinberg, R. A., McWherter, C. A., Freeman, S. K., Wood, D. C., Gordon, J. I., and Lee, S. C. (1995) *Mol. Microbiol. 16*, 241−250.
15. Lodge, J. K., Jackson-Machelski, E., Toffaletti, D. L., Perfect, J. R., and Gordon, J. I. (1994) *Proc. Natl. Acad. Sci. U.S.A. 91*, 12008−12012.
16. Lodge, J. K., Jackson-Machelski, E., Higgins, M., McWherter, C. A., Sikorski, J. A., Devadas, B., and Gordon, J. I. (1998) *J. Biol. Chem. 273*, 12482−91.
17. Lodge, J. K., Johnson, R. L., Weinberg, R. A., and Gordon, J. I. (1994) *J. Biol. Chem. 269*, 2996−3009.
18. Gunaratne, R. S., Sajid, M., Ling, I. T., Tripathi, R., Pachebat, J. A., and Holder, A. A. (2000) *Biochem. J. 348*, 459−63.
19. Qi, Q., Rajala, R. V., Anderson, W., Jiang, C., Rozwadowski, K., Selvaraj, G., Sharma, R., and Datla, R. (2000) *J. Biol. Chem. 275*, 9673−83.
20. Zhang, L., Jackson-Machelski, E., and Gordon, J. I. (1996) *J. Biol. Chem. 271*, 33131−40.
21. Adams, M. D., Celniker, S. E., Holt, R. A., Evans, C. A., Gocayne, J. D., Amanatides, P. G., Scherer, S. E., Li, P. W., Hoskins, R. A., Galle, R. F., George, R. A., Lewis, S. E., Richards, S., Ashburner, M., Henderson, S. N., Sutton, G. G., Wortman, J. R., Yandell, M. D., Zhang, Q., Chen, L. X., Brandon, R. C., Rogers, Y. H., Blazej, R. G., Champe, M., Pfeiffer, B. D., Wan, K. H., Doyle, C., Baxter, E. G., Helt, G., Nelson, C. R., Gabor Miklos, G. L., Abril, J. F., Agbayani, A., An, H. J., Andrews-Pfannkoch, C., Baldwin, D., Ballew, R. M., Basu, A., Baxendale, J., Bayraktaroglu, L., Beasley, E. M., Beeson, K. Y., Benos, P. V., Berman, B. P., Bhandari, D., Bolshakov, S., Borkova, D., Botchan, M. R., Bouck, J., Brokstein, P., Brottier, P., Burtis, K. C., Busam, D. A., Butler, H., Cadieu, E., Center, A., Chandra, I., Cherry, J. M., Cawley, S., Dahlke, C., Davenport, L. B., Davies, P., de Pablos, B., Delcher, A., Deng, Z., Mays, A. D., Dew, I., Dietz, S. M., Dodson, K., Doup, L. E., Downes, M., Dugan-Rocha, S., Dunkov, B. C., Dunn, P., Durbin, K. J., Evangelista, C. C., Ferraz, C., Ferriera, S., Fleischmann, W., Fosler, C., Gabrielian, A. E., Garg, N. S., Gelbart, W. M., Glasser, K., Glodek, A., Gong, F., Gorrell, J. H., Gu, Z., Guan, P., Harris, M., Harris, N. L., Harvey, D., Heiman, T. J., Hernandez, J. R., Houck, J., Hostin, D., Houston, K. A., Howland, T. J., Wei, M. H., Ibegwam, C., et al. (2000) *Science 287*, 2185−95.
22. Giang, D. K., and Cravatt, B. F. (1998) *J. Biol. Chem. 273*, 6595−8.
23. Towler, D. A., Adams, S. P., Eubanks, S. R., Towery, D. S., Jackson-Machelski, E., Glaser, L., and Gordon, J. I. (1987) *Proc. Natl. Acad. Sci. U.S.A. 84*, 2708−2712.
24. Kishore, N. S., Lu, T., Knoll, L. J., Katoh, A., Rudnick, D. A., Mehta, P. P., Devadas, B., Huhn, M., Atwood, J. L., Adams, S. P., Gokel, G. W., and Gordon, J. I. (1991) *J. Biol. Chem. 266*, 8835−8855.
25. Rudnick, D. A., Lu, T., Jackson-Machelski, E., Hernandez, J. C., Li, Q., Gokel, G. W., and Gordon, J. I. (1992) *Proc. Natl. Acad. Sci. U.S.A. 89*, 10507−10511.
26. Johnson, D. R., Cok, S. J., Feldmann, H., and Gordon, J. I. (1994) *Proc. Natl. Acad. Sci. U.S.A. 91*, 10158−10162.
27. Devadas, B., Zupec, M. E., Freeman, S. K., Brown, D. L., Nagarajan, S., Sikorski, J. A., McWherter, C. A., Getman, D. P., and Gordon, J. I. (1995) *J. Med. Chem. 38*, 1837−40.
28. Devadas, B., Freeman, S. K., McWherter, C. A., Kishore, N. S., Lodge, J. K., Jackson-Machelski, E., Gordon, J. I., and Sikorski, J. A. (1998) *J. Med. Chem. 41*, 996−1000.
29. McWherter, C. A., Rocque, W. J., Zupec, M. E., Freeman, S. K., Brown, D. L., Devadas, B., Getman, D. P., Sikorski, J. A., and Gordon, J. I. (1997) *J. Biol. Chem. 272*, 11874−11880.
30. Sikorski, J. A., Devadas, B., Zupec, M. E., Freeman, S. K., Brown, D. L., Lu, H. F., Nagarajan, S., Mehta, P. P., Wade, A. C., Kishore, N. S., Bryant, M. L., Getman, D. P., McWherter, C. A., and Gordon, J. I. (1997) *Biopolymers 43*, 43−71.
31. Rudnick, D. A., McWherter, C. A., Rocque, W. J., Lennon, P. J., Getman, D. P., and Gordon, J. I. (1991) *J. Biol. Chem. 266*, 9732−9.
32. Rocque, W. J., McWherter, C. A., Wood, D. C., and Gordon, J. I. (1993) *J. Biol. Chem. 268*, 9964−9971.
33. Bhatnagar, R. S., Jackson-Machelski, E., McWherter, C. A., and Gordon, J. I. (1994) *J. Biol. Chem. 269*, 11045−53.
34. Bhatnagar, R. S., Schall, O. F., Jackson-Machelski, E., Sikorski, J. A., Devadas, B., Gokel, G. W., and Gordon, J. I. (1997) *Biochemistry 36*, 6700−8.
35. Weston, S. A., Camble, R., Colls, J., Rosenbrock, G., Taylor, I., Egerton, M., Tucker, A. D., Tunnicliffe, A., Mistry, A., Mancia, F., de la Fortelle, E., Irwin, J., Bricogne, G., and Pauptit, R. A. (1998) *Nat. Struct. Biol. 5*, 213-21.
36. Bhatnagar, R. S., Futterer, K., Farazi, T. A., Korolev, S., Murray, C. L., Jackson-Machelski, E., Gokel, G. W., Gordon, J. I., and Waksman, G. (1998) *Nat. Struct. Biol. 5*, 1091−7.
37. Modis, Y., and Wierenga, R. (1998) *Structure 6*, 1345−50.
38. Dutnall, R. N., Tafrov, S. T., Sternglanz, R., and Ramakrishnan, V. (1998) *Cell 94*, 427−38.
39. Rojas, J. R., Trievel, R. C., Zhou, J., Mo, Y., Li, X., Berger, S. L., Allis, C. D., and Marmorstein, R. (1999) *Nature 401*, 93−8.
40. Angus-Hill, M. L., Dutnall, R. N., Tafrov, S. T., Sternglanz, R., and Ramakrishnan, V. (1999) *J. Mol. Biol. 294*, 1311−25.
41. Clements, A., Rojas, J. R., Trievel, R. C., Wang, L., Berger, S. L., and Marmorstein, R. (1999) *EMBO J. 18*, 3521−32.
42. Lin, Y., Fletcher, C. M., Zhou, J., Allis, C. D., and Wagner, G. (1999) *Nature 400*, 86−9.
43. Sternglanz, R., and Schindelin, H. (1999) *Proc. Natl. Acad. Sci. U.S.A. 96*, 8807−8.
44. Trievel, R. C., Rojas, J. R., Sterner, D. E., Venkataramani, R. N., Wang, L., Zhou, J., Allis, C. D., Berger, S. L., and Marmorstein, R. (1999) *Proc. Natl. Acad. Sci. U.S.A. 96*, 8931−6.
45. Wybenga-Groot, L. E., Draker, K., Wright, G. D., and Berghuis, A. M. (1999) *Struct. Fold Des. 7*, 497−507.
46. Wolf, E., Vassilev, A., Makino, Y., Sali, A., Nakatani, Y., and Burley, S. K. (1998) *Cell 94*, 439−49.
47. Hickman, A. B., Klein, D. C., and Dyda, F. (1999) *Mol. Cell 3*, 23−32.
48. Hickman, A. B., Namboodiri, M. A., Klein, D. C., and Dyda, F. (1999) *Cell 97*, 361−9.
49. Duronio, R. J., Jackson-Machelski, E., Heuckeroth, R. O., Olins, P. O., Devine, C. S., Yonemoto, W., Slice, L. W., Taylor, S. S., and Gordon, J. I. (1990) *Proc. Natl. Acad. Sci. U.S.A. 87*, 1506−10.
50. Edelhoch, H. (1967) *Biochemistry 6*, 1948−54.
51. Passonneau, J. V., and Lowry, O. H. (1993) *Enzymatic Analysis*, Humana Press, Totowa, NJ.

52. Parker, C. A. (1968) *Photoluminescence of Solutions*, Elsevier Scientific Publishing, Co., Amsterdam.
53. Johnson, K. A. (1992) in *The Enzymes*; pp 1−60, Academic Press, Inc.
54. Cyert, M. S., and Thorner, J. (1992) *Mol. Cell Biol. 12*, 3460−9.
55. Paige, L. A., Zheng, G. Q., DeFrees, S. A., Cassady, J. M., and Geahlen, R. L. (1989) *J. Med. Chem. 32*, 1665−7.
56. Zimmerle, C. T., Patane, K., and Frieden, C. (1987) *Biochemistry 26*, 6545−52.
57. De Angelis, J., Gastel, J., Klein, D. C., and Cole, P. A. (1998) *J. Biol. Chem. 273*, 3045−50.
58. Khalil, E. M., De Angelis, J., and Cole, P. A. (1998) *J. Biol. Chem. 273*, 30321−7.

BI002074T